Table of contents

Volume 2739

2024

← Previous issue Next issue →

3rd International Symposium on Advances and Innovation in Mechanical Engineering (ISAIME 2022) 13/10/2022 - 14/10/2022 Makassar, Indonesia

Accepted papers received: 27 March 2024
Published online: 18 April 2024

Open all abstracts

Preface

Energy

View article PDF

OPEN ACCESS 012003

Analysis of the Characteristics of Rice Husk and Pinecone Bio-briquettes with Tapioca Flour Adhesive

D Suanggana, C Qalbi AM, F Fijatmoko and GA Duma

View article PDF

OPEN ACCESS 012004

Analysis of Solar Water Heater with Modification Absorber Plate Integrated Thermal Storage

M A I Rahmadhani, Jalaluddin and A A Mochtar

View article PDF

OPEN ACCESS 012005

Potential Torrefaction of Tropical Forest Fruits Waste

H Prayitno, Amrul, R Lestari and R Kurniawansah

View article PDF

OPEN ACCESS 012006

An Effect of Gap Ratios at Four Circular Cylinders in a Staggered Configuration Near a Plane Wall

A G Wailanduw and T Yuwono

View article PDF

OPEN ACCESS 012007

Two-Phase Flow Patterns of Air – Water and Oil in Mini Channel Against Horizontal Position

Sukamta, Z A Faiz, Sudarja and S Sundari

View article PDF

OPEN ACCESS 012008

The Effect of Use of Adhesive to Calorific Value Cymbopogon Nardus Waste Briquettes

N Hendri, D Y Sari, Wagino, D Sakti and A Ramadhan

View article PDF

OPEN ACCESS 012009

Equilibrium Volumetric Experiment Apparatus Review for Mixed-Gas Adsorption

R Huwae, M Nuriyadi, AT. Tjiptadi and Nasruddin

View article PDF

OPEN ACCESS 012010

Effect of Hydroxy Gas Addition in Gasoline-ethanol Fuel Mixture on Performance of Spark Ignition Engine

A Rahman, Asnawi, R Putra, N Islami and H Radian

View article PDF

OPEN ACCESS 012011

Thermodynamic Simulation of Cascade Cooling System for Vacuum Freeze Drying

I Buana and E A Kosasih

View article PDF

OPEN ACCESS 012012

Return Air Grille Position in a Cleanroom for Medicinal Packaging Using CFD Method

L Lestari and R Permatasari

View article PDF

OPEN ACCESS 012013

Experimental Study on Flame Merging Phenomenon

S D Famaretha, M A Santoso and Y S Nugroho

View article PDF

OPEN ACCESS 012014

Microchannel-based Droplet Generation Using Multiphase Flow: A Review

K Raynaldo, Y Whulanza and R Irwansyah

View article PDF

OPEN ACCESS 012015

Thermal Performance of Hybrid PV/T-TEC Air Collector with Perforated-Finned Absorber Plate

Amrizal, Amrul, M H Akram, A Yonanda and M Irsyad

View article PDF

OPEN ACCESS 012016

Biodiesel Production Process Using Plasma Method on Engine Performance and Exhaust Gas Emissions

N Azis, N Amaliyah, A E E Putra, D Kusumawati and M Aldi

View article PDF

OPEN ACCESS 012017

Application of Soy Wax Phase Change Material as Thermal Energy Storage in Wall Building

T Trisnadewi and N Putra

View article PDF

OPEN ACCESS 012018

Thermal Properties Characteristic of Aluminium-Alumina Composite for Solar Water Heating System Application

Muhammad Hasan Basri, Jalaluddin, Rustan Tarakka, Muhammad Syahid, Andi Amijoyo Mochtar and M. Anis Ilahi Ramadhani

View article PDF

OPEN ACCESS 012019

Biogas Production in a Variety of Sawdust and Cow Dung Mixtures Using the Intermittent Mixing Method

A A Mochtar, Jalaluddin, A Mangkau, A Sakka, I Aqsa and M Khoir

View article PDF

OPEN ACCESS 012020

Analysis of Characteristics of Bamboo Water Wheels 6 Bamboo Plate with Height Variations of Water Attacking the Blade

Luther Sule, Andi Amijoyo Mochtar, Andi Mangkau and Elieser Timbayo Sule

View article PDF

OPEN ACCESS 012021

Experimental Study of the Influence of Flap Angle Configuration on the Drag Coefficient of Airfoil Model of Homebuilt Aircraft

N Salam, R Tarakka, L Kasim and M A Wahab

View article PDF

OPEN ACCESS 012022

Development of a New Model "MAGIC BOILER" for Faster Steam Production

S A Aristiana, I Roihan and R A Koestoer

View article PDF

Advanced Material

OPEN ACCESS 012023

Surface Roughness Analysis and Optimization for ST 37 Steel in Lathe Operation using Design of Experiments Method

Anis Siti Nurrohkayati, Sabaruddin Syach and Muhammad Takdir

View article PDF

OPEN ACCESS 012024

Effect of Tool Profile on Mechanical Properties, Temperature, and RPM Using Micro Friction Stir Spot Welding (mFSSW) on Aluminum Alloy AA1100

L A Safitri, I F Fakhrurrozi, M A Amat, A S Baskoro, P Rupajati and G Kiswanto

View article PDF

OPEN ACCESS 012025

The Effect of Welding Process Parameters on the nilon-6 Plate Friction Stir Welded Joint

A W Nugroho, I Aulistianto and C Budiyantoro

View article PDF

OPEN ACCESS 012026

Effect of Pad Thickness and Width Variations on Plastic Limit Moment in Cylindrical Pressure Vessels Due to Nozzle In-Plane Load

R. Nurdin and R. Sriwijaya

View article PDF

OPEN ACCESS 012027

Identification of Water Hyacinth Fiber (Eichornia Crassipes) and Polyethylene Terephthalate Waste as an Alternative Material

S Junus, R F Uloli, F A Rauf, I Renreng, M Syahid, A Hayat and H Uloli

View article PDF

OPEN ACCESS 012028

Analysis of 3D-Printing Layer Height Pattern Effect to ADC12's Mechanical Properties Investment Casting Results

W Suprapto, Y S Irawan and P Auliasyah

View article PDF

OPEN ACCESS 012029

Effect of Austempering Holding Time Variations of 30, 60, and 90 Minutes at 300 °C on The Microstructure and Toughness of Nodular Cast Iron

A S Darmawan, A D Anggono, A Yulianto, B W Febriantoko and A Hamid

View article PDF

OPEN ACCESS 012037

Social Parameter's Role in BEM-PSO-Based Inverse Analysis for Locating Corrosion of Reinforced Concrete

S Fonna, I B M Ibrahim, A Julianda, R Kurniawan, S Huzni and A K Ariffin

View article PDF

OPEN ACCESS 012038

The effect of temperature variation on Aluminum Matrix Composite (AMC) Sintering with CNT

S Salu, I Renreng, M Syahid and A A Mochtar

View article PDF

OPEN ACCESS 012039

Simulation of Static Loading of Electric Tricycle Frame

M Syahid, A Rudi, A Hayat, L Kasim, A A Mochtar and M Ansar

View article PDF

OPEN ACCESS 012040

The Effect Analysis of ZnO Variations on Corn Starch and Cellulose Biocomposites toward Impact Strength

I K A Widi, T A Sutrisno, R Febritasari and A Ariyanto

View article PDF

OPEN ACCESS 012041

The Effect of Welding Current on Shear Test and Microstructure TIG Brazing of Cemented Carbide and Steel

Fadelan, Y Winardi, W T Putra and T P Anangga

View article PDF

OPEN ACCESS 012042

Investigation of surface roughness and tool wear in milling of AISI 4340 steel

A Y Aminy, H Arsyad, Fahri and A Hayat

View article PDF

OPEN ACCESS 012043

Metallurgical Characterization of Micro Friction Stir Spot Welding (μFSSW) Parameters on Similar Materials AA1100

S B Membala, O S Sutresman, H Arsyad, M Syahid and A Widyianto

View article PDF

OPEN ACCESS 012044

Effect of Welding Time Variation in Resistance Spot Welding on Mechanical Properties of Dissimilar Joints on Mild Steel and AISI 304 Stainless Steel

K Pasau, N Salam, A Y Aminy and A Hayat

View article PDF

OPEN ACCESS 012045

The Limit of Incomplete Information in Inverse Analysis for Hidden Corrosion Inference in Reinforced Concrete

I B M Ibrahim, S Fonna, R Kurniawan and S Huzni

View article PDF

Design and Applied Mechanics

OPEN ACCESS 012046

The Effect of Contact Model on Stress Distribution on Internal Fixation of Fibula Fracture

S Huzni, F Rahiem, S Fonna, I B M Ibrahim and AK Arifffin

View article PDF

OPEN ACCESS 012047

Cell Design in Crash Box to Increase the Energy Absorption Efficiency

M M Harbelubun, W Hardi and K Umar

View article PDF

OPEN ACCESS 012048

Finite Element Analysis of Polyethylene Pipe with Elliptical Hole Supported by Saddle Fusion Patch with Fin

T L Hermawan and R Sriwijaya

View article PDF

OPEN ACCESS 012049

Experimental Study of Strain Measurement using 2D Digital Image Correlation on Fixation Plate and Calcaneus Bone Fracture

I Irwansyah, M Dirhamsyah, E Iswardy, T Nanta Aulia, M Alkindi and S N Diah Fitriani

View article PDF

OPEN ACCESS 012050

Development of Two Wheel Drive Electric Bikes for Extreme Road and A Long-Range Capabilities

S Candra, S Tjandra, A Soesanti, H Susanto and T W Prihartono

View article PDF

OPEN ACCESS 012051

Development of Amplitude Measurement System for Ultrasonic Vibration Assisted Micro Forming

G Kiswanto, S T Dwiyati, R A Adityawarman, E J P Mendrofa, H T Tjong and W Z Abdurrohman

View article PDF

OPEN ACCESS 012052

High-Speed Train Running Characteristics Assessments Using Multibody Dynamics Simulation

E D J Putra, Y A Handoko, P Wikaranadhi and J M Valentino

View article PDF

OPEN ACCESS 012053

Study on Design of Hybrid Diesel-Electric Motor Propulsion System for Eco-Tourism Boat

Muhammad Arif Budiyanto, Mohammad Zyan Beckham, Gerry Liston Putra and Achmad Riadi

View article PDF

OPEN ACCESS 012054

Railway track vertical irregularities classification based on vehicle response using machine learning method

P Wikaranadhi, S D Alfian, Y A Handoko and P S Palar

View article PDF

OPEN ACCESS 012055

Procedure in developing a longitudinal-torsional vibration-assisted micro-milling system

G Kiswanto, A M Fahmi, Z Hasymi, M A Atmadja and M N A Perdana

View article PDF

OPEN ACCESS 012056

Comparison Industry 4.0 Assessment Reference Standards to Develop an Assessment Tool Industry 4.0

M R Araliz, H S Nugroho and B Ibrahim

View article PDF

JOURNAL LINKS

Journal home

PAPER • OPEN ACCESS

Preface

Journal of Physics: Conference Series, Volume 2739, 3rd International Symposium on Advances and Innovation in Mechanical Engineering (ISAIME 2022) 13/10/2022 - 14/10/2022 Makassar, Indonesia

Citation 2024 *J. Phys.: Conf. Ser.* **2739** 011001

DOI 10.1088/1742-6596/2739/1/011001

Abstract

It is a great privilege for us to present the proceedings of ISAIME 2022 to the authors and delegates of the event. International Symposium on Advances and Innovation in Mechanical Engineering (ISAIME) is an international conference initiated by Badan Kerja Sama Teknik Mesin (BKSTM), the Indonesian National Organization on Mechanical Engineering. This event is hosted by the Mechanical Engineering Department, Hasanuddin University, Makassar, and held in Makassar, Indonesia on October, 13th 2022. This conference is an invaluable opportunity for academia and researchers to present and publish their works on the advancement of mechanical engineering and technologies

ISAIME conference has three broad topics namely energy, advanced material, and design and applied mechanics. On this occasion, there were four distinguished keynote speakers and oral presentations by participants which brought great opportunities to share their recent research works and knowledge with each other.

Peer review committees tirelessly delivered constructive critical comments to the authors to improve the quality of the presented papers. We are very grateful to the keynote speakers, reviewers, advisory committee, session chairs, and all the authors for their active participation and principal contribution to the success of this conference. We would also like to extend our thanks to the members of the organizing team for their hard work.

List of Editors, Steering Committee, Advisory Board/Reviewer, Organizing Committee are available in this Pdf.

Preface

View PDF

Journal of Physics:
Conference Series

PAPER • **OPEN ACCESS**

Peer Review Statement

To cite this article: 2024 *J. Phys.: Conf. Ser.* **2739** 011002

Peer Review Statement

1. Type of peer review: Single anonymous
2. Conference submission management system: Morressier
3. Number of submissions received: 90
4. Number of submissions sent for review: 90
5. Number of submissions accepted: 56
6. Acceptance Rate (Submissions Accepted / Submissions Received × 100): 62.2 %
7. Average number of reviews per paper: 1.11
8. Total number of reviewers involved: 7
9. Contact person for queries:
   Name: Novriany Amaliyah
   Affiliation: Hasanuddin University
   Email: novriany@unhas.ac.id

PAPER • OPEN ACCESS

Return Air Grille Position in a Cleanroom for Medicinal Packaging Using CFD Method

L Lestari[1] and R Permatasari[1]

Published under licence by IOP Publishing Ltd

Journal of Physics: Conference Series, Volume 2739, 3rd International Symposium on Advances and Innovation in Mechanical Engineering (ISAIME 2022) 13/10/2022 - 14/10/2022 Makassar, Indonesia

Citation L Lestari and R Permatasari 2024 *J. Phys.: Conf. Ser.* **2739** 012012

DOI 10.1088/1742-6596/2739/1/012012

rosyida@trisakti.ac.id

[1] Department of Mechanical Engineering, Faculty of Industrial Technology, Universitas Trisakti

Abstract

A cleanroom is a highly controlled environment; therefore, air quality is of significant concern, and specific physical and microbiological requirements must meet the standard. In addition to the number of particles, another critical parameter in a cleanroom is temperature. USP (The United States Pharmacopeia) 797 recommends that the temperature of a cleanroom be around 20 °C. Air quality is achieved through several parameters and components, such as using a high-efficiency particulate air filter (HEPA), the amount of fresh air entering the room, temperature, pressure

difference, and airflow direction. In this study, the cooling load of the room for the filling and sealing process was calculated, and the airflow and temperature distribution patterns between two parameters of the return air grille (RAG) position were compared using Computational Fluid Dynamics (CFD). The first parameter, RAG 1, was placed above the ceiling, while the second parameter, RAG 2, was set on the sidewall. Based on the results of the study, it was found that the heat load generated from the room was 6.99 kW with a cooling coil capacity amounting to 10.77 kW. Moreover, the supply airflow rate was 371.66 l/s. Based on the results of the simulation modelling, it was found that the RAG positioned on the sidewall was more ideal than the RAG positioned above the ceiling since the temperature was more evenly distributed in the room where the RAG was positioned on the sidewall.

Development of Evaluation Method for Organic Contamination on Silicon Wafer Surfaces

View PDF

Journal of Physics:
Conference Series

PAPER • **OPEN ACCESS**

Return Air Grille Position in a Cleanroom for Medicinal Packaging Using CFD Method

To cite this article: L Lestari and R Permatasari 2024 *J. Phys.: Conf. Ser.* **2739** 012012

Return Air Grille Position in a Cleanroom for Medicinal Packaging Using CFD Method

L Lestari and R Permatasari*

Department of Mechanical Engineering, Faculty of Industrial Technology, Universitas Trisakti

*rosyida@trisakti.ac.id

Abstract. A cleanroom is a highly controlled environment; therefore, air quality is of significant concern, and specific physical and microbiological requirements must meet the standard. In addition to the number of particles, another critical parameter in a cleanroom is temperature. USP (The United States Pharmacopeia) 797 recommends that the temperature of a cleanroom be around 20 °C. Air quality is achieved through several parameters and components, such as using a high-efficiency particulate air filter (HEPA), the amount of fresh air entering the room, temperature, pressure difference, and airflow direction. In this study, the cooling load of the room for the filling and sealing process was calculated, and the airflow and temperature distribution patterns between two parameters of the return air grille (RAG) position were compared using Computational Fluid Dynamics (CFD). The first parameter, RAG 1, was placed above the ceiling, while the second parameter, RAG 2, was set on the sidewall. Based on the results of the study, it was found that the heat load generated from the room was 6.99 kW with a cooling coil capacity amounting to 10.77 kW. Moreover, the supply airflow rate was 371.66 l/s. Based on the results of the simulation modelling, it was found that the RAG positioned on the sidewall was more ideal than the RAG positioned above the ceiling since the temperature was more evenly distributed in the room where the RAG was positioned on the sidewall.
Keywords: *Cleanroom, Return Air Grille, CFD.*

1. Introduction

A cleanroom is used in treating patients at a hospital, examining, and manufacturing a product in several industries such as microelectronics, pharmacy, biotechnology, medical equipment, and food and beverages. A cleanroom is a closed room capable of providing control over particulate contamination in the air. Particulate contamination may be either in the form of a micro-organism such as bacteria, microbes, or viruses in the form of a non-living particle such as metal, organic or inorganic compounds, pollution, or dust [1]. ISO 14644-1 stipulates that the permissible particulate size for the cleanroom area ranges from 0.1 µm to 5 µm [2]. In addition to the number of particles, another critical parameter in a cleanroom is temperature. USP (The United States Pharmacopeia) 797 recommends that the temperature of a cleanroom be around 20 °C [3].

The air pattern of the cleanroom is affected by the configuration of air supply, return air, and its flow rate. When designing a good cleanroom, the first step that should take is selecting the configuration of the air pattern [1]. An appropriately designed air pattern will result in evenly distributed cold air in the room.

Bishnoi and Aharwal (2019) did a study on the effects of an airflow plane in the room and concluded that the airflow and temperature distribution impacted on the optimization [4].

The airflow pattern and the temperature distribution may depend on several inter-related factors such as the RAG position, airflow rate, air temperature, and the number of particulates in the cleanroom. A physical examination and measurement to study the effects of all these factors on thermal comfort, energy efficiency, and the level of hygiene will take such a long time. In this situation, analyzing various realistic scenarios through Computational Fluid Dynamics (CFD) method serves as an interesting alternative [5]. The results of CFD may be presented in a color contour plot as shown by Fig. 1. It shows the temperature distribution and particle concentration in a cleanroom. An airflow path line and a vector plot are employed to show the airflow pattern in the cleanroom. A flow animation also helps visualize the movement of air and particles in the cleanroom.

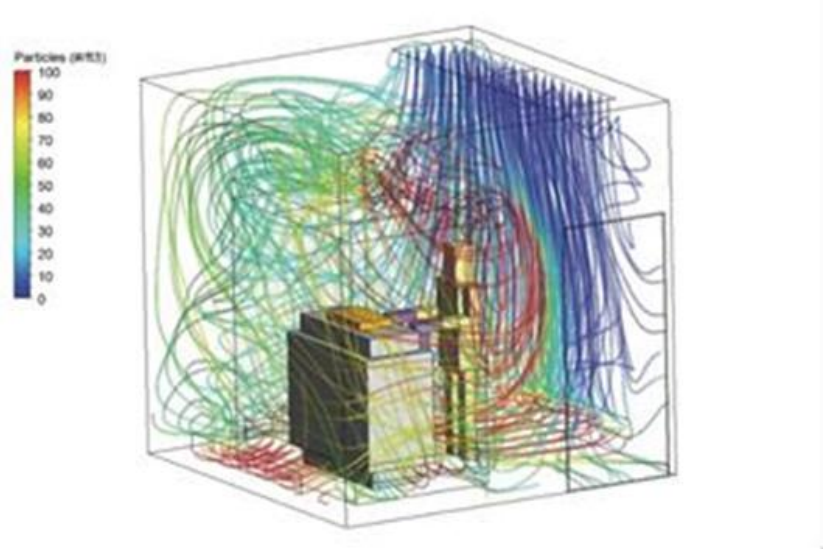

Figure 1. Airflow Pattern Simulation [1]

A CFD analysis can predict the generated airflow pattern and temperature distribution, the concentration of particles, the relative humidity distribution, and the occupant's thermal comfort in a confined space such as a cleanroom. Bagus Satrio (2020) analyzed the temperature distribution of a computer laboratory by considering the thermal comfort of the laboratory. Based on the CFD analysis, it was found out that the airflow pattern could spread to every corner of the computer laboratory, so the cold air was evenly distributed in that room [6].

In this study, calculating the cooling load in the cleanroom and compare the return air grille (RAG) positions for the filling and sealing process of the drugs. The RAG positioned above the ceiling served as the first parameter, and RAG positioned on the sidewall served as the second parameter. Using a CFD method with ANSYS software to obtain the airflow based on these two parameters, could find the most appropriate RAG position producing the airflow, so a good temperature distribution pattern in the room could be achieved.

2. Method

In the implementation, the cooling load in the room was calculated and designed an RAG position with two parameters to be examined. The room to be used in this study was the Filling 2 room in CSAS building intended to produce cough medicines.

2.1. Room Condition

The room serving as the object of study was a 18-square-meter room used in the sealing and filling process for the production of cough medicines. Table 1 shows the condition of the space design.

Table 1. Room Condition

No	Detail	Information
1	Dimension of the Room	6 m by 3 m by 2.75 m
2	Position	Second Floor CSAS L19 Building
3	Location	Tangerang, Banten
4	Design Temperature	20 ℃
5	Room RH	±60%
6	Room Pressure	+
7	Pressure Difference	5 Pa
8	Ambient Temperature	34℃
9	Ambient RH	±80%

The room was located on the second floor of CSAS L19 building as elaborated in Attachment 2. The room was located between the Filling 1 room and the corridor. Fig. 2 showed that the room consisted of three partition walls and the outer wall, where the outer wall faced southward. It showed also the floor plan of the room that was designed with four diffuser supplies and two RAGs. The room temperature was set at 20 ℃ pursuant to USP 797 recommendation, where the cleanroom temperature was around 20 °C [3]. The room was designed to be a room with positive pressure to avoid any air-borne contamination from the other rooms. The pressure difference between Filling 2 room and the other rooms was 5 Pa, pursuant to ISO 14644-4 stipulating that the pressure difference between the clean room should range from 5 to 20 Pa [2].

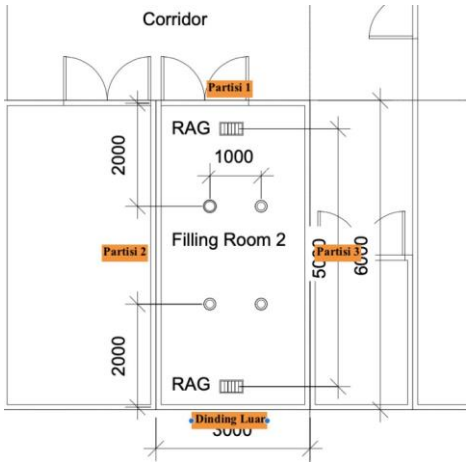

Figure 2. Floor Plan and Positions of the Walls and the Room Partitions

2.2. Cooling Load The Room

The cooling load is generated from various kinds of heat transfers such as conduction, convection, and radiation through the building components and from the internal sources. The building components capable of affecting the cooling load include:

1. External load: Heat load through the walls, roof, windows, doors, partition, ceilings, and floor.
2. Internal: Lamps, people, electronic devices producing heat.

2.3. Infiltration: Air leaks and humidity migration.

The cooling load was calculated by employing a cooling load temperature differential (CLTD) method pursuant to ASHRAE (American Society of Heating, Refrigerating and Air-Conditioning Engineers) standard [7]. CLTD is a theoretical temperature differential calculating the joint effects of the inside and the outside air temperatures, daily temperature range, solar radiation, and thermal storage in the construction [8]. In terms of CLTD value, a CLTDc (Cooling Load Temperature Differential corrected) was obtained, in which CLTDc is a value of temperature differential having been adjusted to the design temperature, the outside temperature, and the latitude of the building.

Below is how the cooling load was calculated through the building, internal and infiltration components:

2.3.1. Heat Load Through The Wall

A wall consists of several different component materials each of which store's heat differently. Moreover, it has its own specific heat properties (Cp) as a measure of the ability of a material to store heat energy [9]. Therefore, a material's thermal conductivity is defined as the rate of a heat transfer through the material thickness unit per unit area per thermal difference unit. The thermal conductivity of a material is a measure of the ability of a material to conduct heat. A high conductivity value indicates that the material is a good conductor of heat, while a low conductivity value indicates that the material is a bad conductor or isolator of heat [10].

The thermal conductivity is calculated use equation (1), where Table 3.11 of Handbook Cooling and Heating Load Calculation Manual ASHRAE shows the thermal resistance value [11].

$$U = 1/ (R1+R2+\ldots+Rn) \quad (1)$$

Where:

U : Heat transfer coefficient, W/m^2K
R : Thermal resistance, $(m^2.K)/W$
x : Material thickness, m

If the wall experiences any contact with the outer air, the value of CLTDc should first be identified. To obtain the value of wall CLTDc, according to ASHRAE Cooling and Heating Load Manual [11] can be calculated use equation (2). Moreover, Table 3.10 of Handbook Cooling and Heating Load Calculation Manual ASHRAE shows the values of CLTD, and Table 3.12 of Handbook Cooling and Heating Load Calculation Manual ASHRAE shows the values of LM [11]:

$$CLTDc = (CLTD + LM) \times K + (25,5-Tr) + (To-29,5) \quad (2)$$

Where:

CLTD : Cooling Load Temperature Difference, °C LM : Latitude Month
K : Coefficient value for the wall color
K : 1.0, for a dark or light color in the industrial area
K : 0.83, for a medium light color in the residential area (light blue, green, etc.)
K : 0.65, for a light color in the residential area (beige)
Tr : Design temperature, °C
To : Outer air temperature, °C

After obtaining the value of CLTDc, the heat load through the wall can be calculated. According to ASHRAE Cooling and Heating Load Manual [11], the heat load is calculated using an equation (3) as follows:

$$Q = U \times A \times CLTDc \quad (3$$

Where:

Q : Wall cooling load, Watt

CLTDc : Cooling Load Temperature Difference Corrected, °C
U : Wall heat transfer coefficient, W/m^{2}K
A : Area of the wall, m^2 .

2.3.2. Heat Load Through The Roof
The value of roof CLTDc is calculated use equation (4), Table 3.8 of ASHRAE Cooling and Heating Load Manual shows the values CLTD, and Table 3.12 of ASHRAE Cooling and Heating Load Manual shows the values of LM [11].

$$CLTDc = (CLTD + LM) \times K + (25.5-Tr) + (To-29.5) \quad (4)$$

Where:
CLTD : Cooling Load Temperature Difference, °C LM : Latitude Month
K : Coefficient value for the roof color
Tr : Design temperature, °C
To : Outside air temperature, °C
The conduction heat color through the roof is calculated with equation (5), and, like the wall and roof, the coefficient value of the heat transfer is calculated use equation (1).

$$Q = U \times A \times CLTDc \quad (5)$$

Where:
Q : Roof cooling load, Watt
CLTDc : Cooling Load Temperature Difference Corrected, °C
U : Wall heat transfer coefficient, W/m^2.
KA : Area of the wall, m^2

2.3.3. Heat Load Through The Floor And The Partition
The conduction heat color through the floor and the partition is calculated use equation (6), and, like the wall and roof, the coefficient value of the heat transfer is calculated with equation (1).

$$Q = U \times A \times \Delta T \quad (6)$$

Where:
Q : Heat load through the Floor/Partition
U : Roof heat transfer coefficient, W/m^{2}K
ΔT : Temperature differential, °C
A : Area of the floor/partition, m^2

2.3.4. Heat Load Through the Lamp
The heat load from the light-bearing equipment is calculated use equation (7). Moreover, Table 4.1 of ASHRAE Cooling and Heating Load Manual shows the values of ballast factors and Table 4.4 of ASHRAE Cooling and HeatingLoad Manual shows the values of CLF [11].

$$Q = qi \times fs \times fu \times CLF \quad (7)$$

Where:
Q : Light cooling load, Watt
qi : Total power of the lamps, Watt
fu : Percentage of lamp usage, %
fs : Ballast factor
CLF : Lamp cooling load factor

2.3.5. Heat Load From the Occupants

Not only do humans produce sensible heat, but they also produce latent heat. Human heat load is calculated to use equations (8) and (9), where Table 4.5 of ASHRAE Cooling and Heating Load Manual shows the values of heat per person [11]. The value of CLF is assumed to be 1 since the air conditioner works less than 24 hours [11].

$$Qs = n \times qs \times CLF \quad (8)$$

Where:

Qs	: Sensible cooling load of the occupant's load, Watt
Ql	: Latent cooling load of the occupant's load, Watt
n	: Number of occupants
qs	: Sensible heat produced by the humans, Watt
ql	: Latent heat produced by the humans, Watt
CLF	: Cooling load factor for humans

2.3.6. Heat Load from Equipment Heat Load

Equipment heat load is calculated using equation (9). Moreover, Table 4.12 of ASHRAE Cooling and Heating LoadManual shows the values of equipment sensible heat, and Table 4.13 of ASHRAE Cooling and Heating Load Manual [11] shows the values of equipment load factor.

$$Qs = qi \times FL \times CLF \quad (9)$$

Where:

Q	: Equipment sensible cooling load, Watt
qi	: Equipment sensible heat, Watt
F_L	: Equipment sensible coefficient
CLF	: Sensible heat factor,
CLF	:1 if the equipment is used less than 24 hours

2.3.7. *Heat Load From Ventilation*

Ventilation is outer air deliberately put in the room in order that the air circulation in the room continues to be maintained. The ventilation heat load is calculated use equations (10) and (11), where Table 5.3 of ASHRAE Coolingand Heating Load Manual shows the occupant's need of air [11]:

$$Qs = 1{,}23 \times \Delta T \times scfm \quad (10)$$

$$Ql = 3.010 \times \Delta W \times scfm \quad (11)$$

Where:

Qs	: Sensible heat load, Watt
Ql	: Latent heat load, Watt Scfm: Occupant's need of air, l/s
ΔT	: Temperature differential between the room air temperature and the outer air temperature, °C
ΔW	: Humidity ratio differential between room humidity and outer air humidity, kg/kg. The air humidity ratio differential is determined with a psychrometric diagram.

2.3.8. *Heat Load Of Infiltration*

Heat can be transmitted through the air entering from a crack in the door or the wall entering the room due to the pressure difference between the rooms, and it occurs naturally. Infiltration air discharge is determined by using the graphs in Fig.3, from the pressure difference and door opening factor (K).

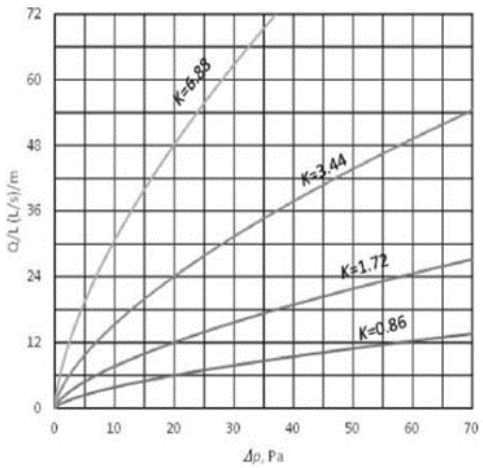

Figure 3. Infiltration Characteristics of the Window and the Door [9]

After obtaining the value of Q/L, the infiltration discharge can be calculated use equation (12).

$$Scfm = P \times Q/L \quad (12)$$

Where:
Scfm : Infiltration air discharge, l/s
P : Perimeter of the door opening, m

The infiltration heat load is calculated use equations (13) and (14).

$$Qs = 1{,}23 \times \Delta T \times scfm \quad (13)$$
$$Ql = 3.010 \times \Delta W \times scfm \quad (14)$$

Where:
Qs : Sensible heat load, Watt
Ql : Latent heat load, Watt
Scfm : Infiltration air discharge, l/s
ΔT : Air temperature differential of the room, °C
ΔW : Ratio differential of the air humidity between the rooms, kg/kg

2.3.9. Psychrometric Analysis

A psychrometric analysis is conducted with psychrometric graphs. There are several parameters on the psychrometric graphs such as the dry air temperature line (T_{db}) serving as the abscissa and the humidity ratio line serving as the ordinate. Mixed air and steam thermodynamics condition will be fully determined if there are three parameter that have been determined [12]. On the psychrometric graph, there are other parameters from the air properties which can help us analyze the air properties such as relative humidity (RH), wet ball temperature, specificvolume, enthalpy, and dew-point temperature. In the psychrometric analysis, we need the comparison value of sensibleheat load to room total load. The value of RSHR is calculated using equation (15).

$$RSHR = RSH/RTH \quad (15)$$

Where:
RSHF : Room sensible heat ratio
RSH : Room sensible heat load (Watt)RLH : room latent heat load (Watt)
RTH : Total sensible and latent heat load (Watt)

The psychrometric graph helps us know the temperature of the room supply in order to determine the capacity ofcooling coil and required supply air discharge. The required supply air discharge is calculated use equation (16).

$$Scfm = RSH/1{,}23 \times (TR - TSA) \quad (16)$$

Where:
scfm : Supply air discharge to the room, l/s
RSH : Room sensible heat load, Watt
T_R : Room temperature, °C
T_{SA} : Supply air temperature, °C

In terms of the capacity of cooling coil pursuant to Handbook Cooling and Heating Load Calculation Manual ASHRAE, the coil capacity is calculated by adding the total oom heat load and sensible and latent heat load of the outside air [11]. The sensible and latent heat load of the fresh air is calculated use equations (17) and (18).

$$OASH = 1{,}23 \times scfmOA \times (TOA - TR) \quad (17)$$
$$OALH = 3.010 \times scfmOA \times (WOA - WR) \quad (18)$$

Whereas:
OASH : outside air heat load, Watt
OALH : outside air heat load, Watt
$Scfm_{OA}$: fresh air discharge, l/s
T_R : room temperature, °C
T_{OA} : outside air temperature, °C
W_R : humidity ratio, kg/kg
W_{OA} : humidity ration, kg/kg

From the air heat load, the required capacity of cooling coil can be calculated use equations (19), (20) and (21).

$$qS = RSH + OALH \quad (19)$$
$$qL = RLH + OALH \quad (20)$$
$$qT = qS + qL \quad (21)$$

3. Results And Discussion

3.1. Calculating the Cooling Load

Tabel 2 shows characteristics of the wall material. The heat transfer coefficient value (U) of the wall is calculated use equation (1), so we obtain results as follows: $Udinding = 1/(Rtotal) = 1/0{,}41 = 2{,}47$ W/m^2 K. The floor on the filling 2 room experienced contact with the roof of the first floor. The floor construction was thesame as the roof construction as shown by Table 3 and Table 4. The heat transfer coefficient value (U) of the roof and the floor was 0.63 W/m^{2}K. The heat transfer coefficient value (U) of the partition was 3.66 W/m^{2}K.

Table 2. Characteristics of the Wall Material

No	Wall Component	Resistance Value (m^2.K)/W
1	Outer Surface Resistance	0.06
2	20-mm Plaster	0,03
3	100-mm Brick	0,14
4	20-mm Plaster	0,03
5	100-mm Polyurethane	0,03
6	Outside air resistance	0,12

Table 3. Material Characteristics of the Roof and the Floor

No	Wall Component	Resistance Value (m^2.K)/W
1	Inner Resistance Value	0.12
2	20-mm Plaster	0.03
3	Concrete	1.17
4	Steel Sliding	0.000035
5	Ceiling Air Space	0.18
6	100-mm Polyurethane	0.03
7	Outer air resistance	0.06

Table 4. Material Characteristics of the Partition

No	Wall Component	Resistance Value (m^2.K)/W
1	Inner Surface Resistance	0,12
2	100-mm Polyurethane	0,03
5	Inner Surface Resistance	0,12

The calculation was conducted based on the data and equations (1) to (21) having been elaborated above as shown inTable 5 and Table 6.

Table 5. Sensible Heat Load

No	Source of Sensible Heat	Equation	Sensible Heat Load (Watt)
1	Heat Load Through the Wall	(2) and (3)	237.15
2	Heat Load Through the Roof	(6)	158.76
3	Heat Load Through the Floor	(6)	158.76
4	Heat Loat Through The Partition	(6)	754.88
5	Heat Load of the Light	(7)	262.66
6	Occupant's Heat Load	(8)	300
7	Equipment Heat Load	(10)	1453.28
8	Heat Load of The Ventilation	(11)	731.42
9	Infiltration Heat Load	(13) and (14)	98.89

Table 6. Latent Heat Load

	Source of Sensible Heat	Equation	Sensible Heat Load (Watt)
1	Occupant's Heat Load	(9)	390
2	Heat Load of The Ventilation	(12)	2.301,31
3	Infiltration Heat Load	(13) and (15)	145.20

Table 7. showed the total heat of the room. It was 6,992.31 Watt. The heat load of the room would be used to calculate the capacity of cooling coil. When calculating the cooling coil, the heat load was added with the safety factor(SF) amounting to 10%.

Table 7. Total Heat Load of the Room

No	Heat Load	Total	Total + SF
1	Sensible Heat (RSH)	4,155.80	4,571.38
2	Latent Heat (RLH)	2,836.51	3,120.16
3	Total Heat (RTH)	6,992.31	7,691.54

3.2. Calculating the Supply Air Discharge to the Room

The air discharge of the air conditioner to the room was calculated use equation (16). Before calculating it, we were required to determine the supply air temperature by using a psychrometric analysis. There are several steps required to use a psychrometric analysis to determine the capacity of cooling coil. They are as follows:

- Plot the air condition and the room air condition in the psychrometric diagram. The outer air condition is marked with point 1 (34 °C and RH amounting to 80%), while the room air condition is marked with point 2 (10 °C and RH amounting to 60%) as shown by Fig. 4.
- Calculate the room sensible heat load ratio value (RSHR) with equation (16), so the results as follows:

  RSHR = 4571.38 Watt/7,691.54 = 0.6 Watt.

  The supply air condition was found when the RSHR line was tangent to the 90-% RH line. Therefore, the requiredsupply air had a temperature amounting to 10 °C, RH amounting to 90%, and humidity ratio amounting to 0.007 kg/kg. The supply air discharge was calculated with equation (16).

  rScfm = 4571.38/1.23 x (20 ℃ – 10 ℃) = 371.66 l/s

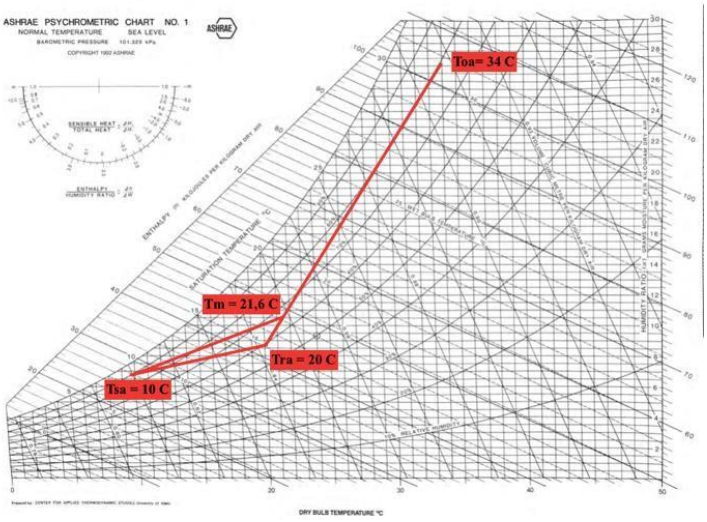

Figure 4. Psychrometric Analysis

3.3. Calculating the Capacity of Cooling Coil

Calculating amount of outside air load with equations (17) and (18) with the outside air discharge amounting to 42.48 l/s, the results as follows:

Sensible heat load of the outside environment:

OASH = 1.23 x 42,48 l/s x (34 ℃ - 20 ℃) = 731.42 W

Latent heat load of the outside environment:

OASH = 3.010 x 42.48 l/s x (0.027 kg/kg – 0.009 kg/kg) = 2,301.31 W

Calculating the capacity of cooling coil of the air conditioner with equations (19), (20) and (21), the results asfollows:

qs = 4,571.38 W + 731.42 W = 5,302.80 W

qL = 3,120.16 W + 2,301.31 W = 5,421.47 W

Hence, the total capacity of cooling coil required to absorb the heat from the outside air was:

qT = 5,302.80 W + 5,421.47 W = 10,724.27 W

3.4. Analyzing the Effects of an RAG Position.

After calculating the cooling load and determining the required numbers of the RAG, then observe the effects of an RAG position on the temperature distribution. The first examination was done with the RAG positioned above theceiling as shown by Figure 5. Moreover, the second examination was done with the RAG positioned on the sidewall as shown by Figure 6.

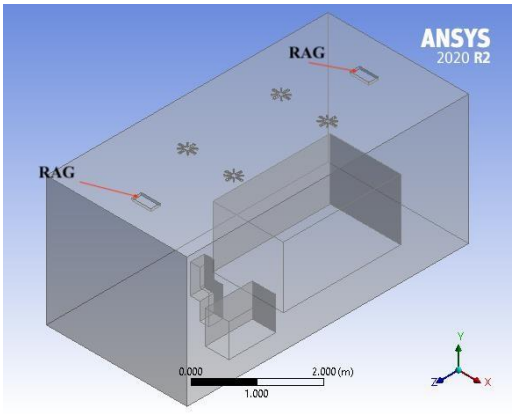

Figure 5. Parameter 1

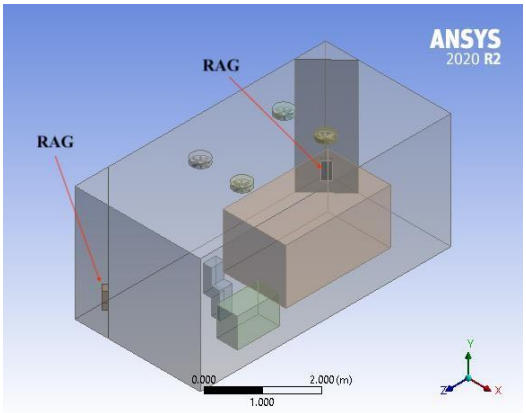

Figure 6. Parameter 2

From those two parameters, comparing the airflows based on the streamline shown by the results of the simulation. Figure 7 shows the airflow of the first parameter, while Figure 8 shows the airflow of the second parameter.

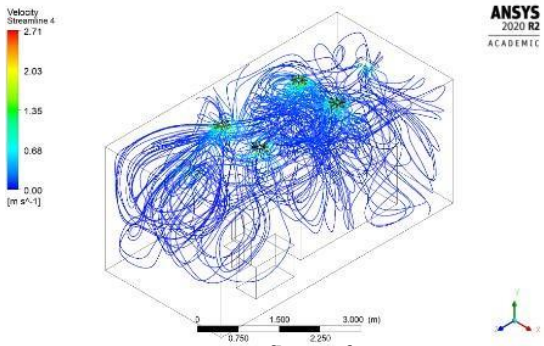

Figure 7. Airflow of Parameter1

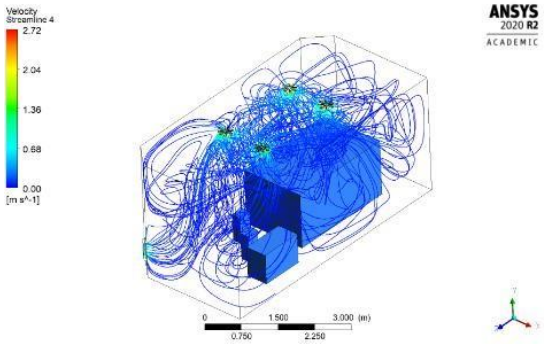

Figure 8. Airflow of Parameter 2

Fig. 7 shows that, in terms of the course of the streamline, the airflow is dominant on the ceiling of the room, while Fig. 8 shows that the airflow reaches every corner of the room. Fig. 9 shows the color contour of the temperature distribution on the ceiling (Y=2.5 m), while the figure on

the right is parameter 1, and the figure on the left is parameter 2. Figure 9 shows that parameter 1 results in a 20℃-air temperature pattern more evenly distributed than that of parameter 2. The 20℃ temperature is depicted with a green contour.

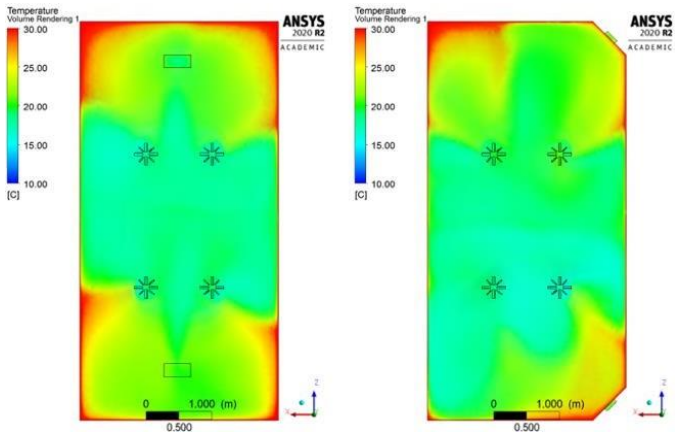

Figure 9. Area Temperature Distribution of the Ceiling (Y>1.5 meter)

Figure 10 shows the temperature distribution at a 1.5-meter altitude above the floor (Y=1.5 m), where 1.5 meters isthe altitude of the air conditioner and the average height of the workers. Fig. 10 shows that the temperature is more evenly distributed in the picture on the left (parameter 2), so it shows us that the airflow pattern affects the temperature distribution, where parameter 1 has a better temperature distribution at a 2.5-meter altitude since the airflow is more dominant on the ceiling as shown by Figure 10. However, at a lower altitude, namely at a 1.5-meter altitude, the temperature distribution of parameter 1 decreases.

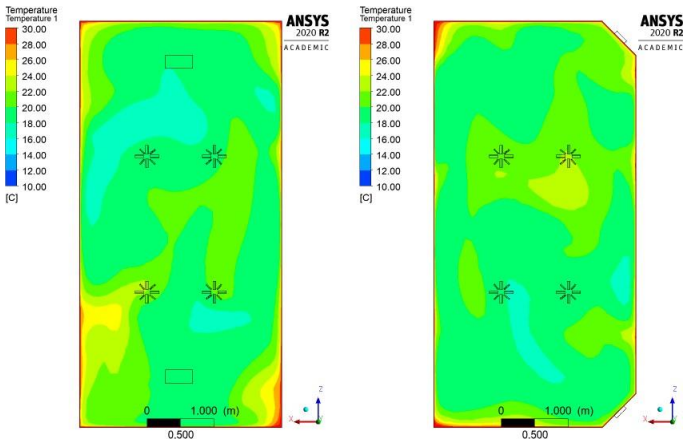

Figure 10. Temperature Distribution of the Ceiling Area (Y=1.5 meter)

Figure 11 shows the temperature distribution from the side of the room at a 1.5-meter altitude. Figure 11 shows that the design of parameter 2 results in a better air distribution, namely the RAG positioned on the sidewall.

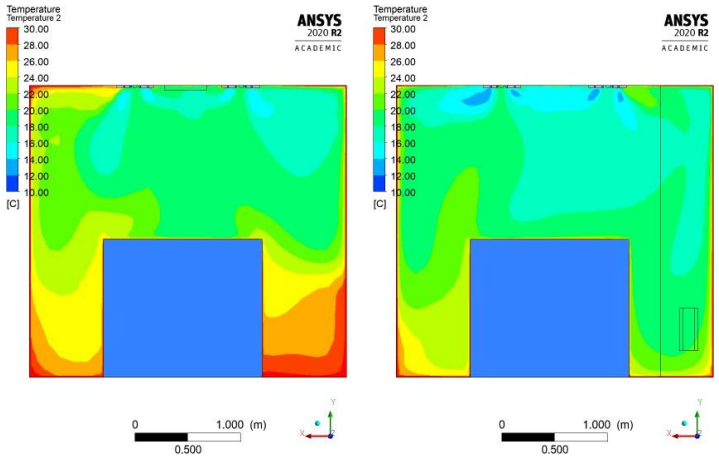

Figure 11. Temperature Distribution from the Side (Z = 2 meter)

Hence, based on the results of the simulation, it is found out that the RAG positioned on the sidewall is more idealthan the RAG positioned on the ceiling since it will result in a more evenly distributed 20 ℃ air; therefore, it will meet the standard SNI and achieve the desired design condition.

4. Conclusion

Based on the results of the study, it is concluded that the heat load of the 6-m-by-3-m-by-2.75-m Filling 2 room is 6.99 kW. The required cooling or the capacity of cooling coil is 10.72 kW with the supply air discharge amounting to 371.77 l/s. Based on the results of the simulation, it is found out that the RAG positioned on the sidewall is the most ideal position since it results in a more evenly distributed temperature than the RAG positioned on the ceiling. The RAG positioned on the sidewall produces the average temperature amounting to 20.59 ℃, while the RAG positioned on the ceiling produces a higher average temperature, namely 20.69 ℃. Hence, it already meets the standards stipulated by ASHRAE for pharmaceutical room.

Acknowledgments

We would like to thank the Department of Mechanical Engineering, Faculty of Industrial Engineering, Universitas Trisakti, which has supported our research.

References

[1] ASHRAE 2017 ASHRAE *Design Guide for Cleanroom Fundamentals* (ASHRAE Inc. Atlanta)
[2] ISO 14644-1 2015 *Classification of Air Cleanliness by Particle Concentration* (ISO, Switzerland)
[3] Gormley T Markel T A Jones III H W Wagner J Greeley D Clarke J H Abkowitz M and Ostojic J 2017 Methodology for analyzing environmental quality indicators in a dynamic operating room environment *American Journal of Infection Control* **45(4)** 354-359
[4] Bisnoi R and Aharwal K 2020 Experimental investigation of air flow field and cooling heterogeneity in a refrigerated room *Engineering Science and Technology, an International Journal*
[5] ASHRAE 2015 *Heating, Ventilating, and Air-Conditioning Applications* (ASHRAE Inc. Atlanta)
[6] Hutomo B S 2020 Calculation of the maximum cooling load and CFD simulation of changes in the velocity of air flowing out of the evaporator on the temperature distribution of the computer laboratory room XYZ Pusdiklat building (FTI - Usakti, Jakarta) (in Bahasa)
[7] ASHRAE 2017 *ASHRAE Fundamentals* (SI Edition), Atlanta
[8] Bhatia A 2014 *Cooling Load Calculations and Principles* (Woodcliff Lake, NJ: Continuing Education and Development, Inc.)
[9] Spitler J D 2014 *Load Calculation Applications Manual 2nd Edition* (Atlanta: ASHRAE)
[10] Cengel Y 2002 *Heat transfer: a practical approach* (New York: McGraw-Hill Science)

[11] Rudoy W 1978 *Handbook Cooling and Heating Load)* Calculation Manual ASHRAE (Atlanta: ASHARE Inc.)
[12] Reddy A T and Kreider F J 2010 *Heating and Cooling of Buildings: Principles and Practice of Energy Efficient Design* (London: CRC Press)
[13] Wiratama J 2020 *Introduction to ANSYS Fluid Simulation Module for Beginners* (Yogyakarta: CV. Markom) (in Bahasa)
[14] Cable M *An Evaluation of Turbulence Models for the Numerical Study of Forced and Natural Convective Flow in Atria* (Canada: Queen's University)